Developments in marine pCO_2 measurement technology; towards sustained *in situ* observations

Jennifer S. Clarke [a, b, *], Eric P. Achterberg [a, b], Douglas P. Connelly [c], Ute Schuster [d], Matthew Mowlem [c]

[a] *Ocean and Earth Sciences, National Oceanography Centre Southampton, University of Southampton, Southampton SO14 3ZH, UK*
[b] *GEOMAR Helmholtz Centre for Ocean Research, 24148 Kiel, Germany*
[c] *National Oceanography Centre, Waterfront Campus, European Way, Southampton SO14 3ZH, UK*
[d] *University of Exeter, North Park Road, Exeter EX4 4QE, UK*

A B S T R A C T

The oceanic uptake of anthropogenic CO_2 causes pronounced changes to the marine carbonate system. High quality pCO_2 measurements with good temporal and spatial coverage are required to monitor the oceanic uptake, identify regions with pronounced carbonate system changes, and observe the effectiveness of CO_2 emission mitigation strategies. There are currently several instruments available, but many are unsuitable for autonomous deployments on *in situ* platforms such as gliders, moorings and Argo floats. We assess currently available technology on its suitability for *in situ* deployment, with a focus on optode technology developments.

Optodes for pCO_2 measurements provide a promising new technological approach, and were successfully calibrated over the range of 280–480 μatm applying modified time-domain dual lifetime referencing. A laboratory precision of 0.8 μatm (n = 10) and a response time (τ_{90}) of 165 s were achieved, and with further development pCO2 optodes may become as widely used as their oxygen counterparts.

© 2017 The Authors. Published by Elsevier B.V. This is an open access article under the CC BY license (http://creativecommons.org/licenses/by/4.0/).

1. Introduction

Atmospheric CO_2 concentrations have increased from 280 μatm in pre-industrial time to daily averages over 400 μatm at Mauna Loa Hawaii in May 2016 [1]. The principle sources of anthropogenic CO_2 for the period 2004–2014 were fossil fuel burning and cement production (8.9 $\pm$ 0.4 Gt C yr^{-1}), and land-use changes (0.9 $\pm$ 0.5 Gt C yr^{-1}) [2]. Atmospheric CO_2 concentrations are expected to continue to increase, with 800 μatm projected by the end of the 21st century [3]. However, less than half of the annual CO_2 emissions remain in the atmosphere; a quarter end up in the ocean, with the remainder absorbed by terrestrial systems [4]. The ocean is thus a major CO_2 sink [5], and therefore is key to our understanding of the global carbon cycle. The wider ecological and biogeochemical impacts from increasing seawater CO_2 are yet to be fully understood, with increasing quantities of data required to improve process understanding [6]. One known consequence of the

oceanic uptake of anthropogenic CO_2, is a decrease in seawater pH with an average reduction of 0.002 pH units per year [7–9]. This CO_2-induced proton release is partially mitigated by the buffering capacity of dissolved bicarbonate and carbonate ions in seawater. However, this buffering capacity is projected to decrease as the anthropogenic CO_2 uptake by the ocean continues [10,11].

The ocean carbonate system can be defined by six variables-Dissolved Inorganic Carbon (DIC), Total Alkalinity (TA), pCO_2, pH, and the concentrations of bicarbonate and carbonate ions [12]. Measurements of any two variables, along with relevant metadata (temperature, salinity, pressure, and nutrients), allow the calculation of the other four. Currently, four of the six carbonate system variables are readily measurable: DIC, TA, pCO_2 and pH, although only pH and pCO2 are analysed routinely *in situ*.

The oceans are strongly under sampled, and sustained autonomous *in situ* observations with sensors are needed to provide enhanced spatial and temporal coverage. Sensors, defined here as deployable *in situ* (i.e. subsurface) analysers, allow measurements on a range of oceanic platforms, and improve both the quantity and quality of data available to facilitate detection of long-term trends. Desirable characteristics for *in situ* chemical sensors include low

cost, low power requirements, ease of integration into platforms, and limited calibration requirements [13]. Whilst shipboard deployments have few constraints on size, power or autonomy, they are expensive to operate, and provide limited temporal and spatial coverage. Gliders and Argo (http://dx.doi.org/10.17882/42182) floats are mobile platforms that travel through the water column at ca. 0.25 m s^{-1} [14] and 0.06 m s^{-1} [15], respectively, and require sensors with small sizes, fast response times and an ability to cope with a range of temperatures and salinities dependent on deployment locations. Moorings and buoys remain at a single location for long periods of time (months to years), and demand longer operational lifetimes for the sensors, but often with less frequent measurements over limited temperature and salinity ranges [16].

2. Sensor technologies for carbon system parameters

The general state of oceanic biogeochemical sensors has been previously reviewed [17–19], and commercially available pCO_2 sensors for use in coastal environments have been evaluated by the Alliance for Coastal Technologies [20].

This paper reviews current technologies for the measurement of open ocean pCO_2. We compare and contrast the existing technologies, and report on the deployment methods for the current generation of sensors, with a discussion on recent developments in optode technology. The metrological data of a range of commonly used commercial sensors is provided in Table 1. Where available, data from peer reviewed journals and the Alliance for Coastal Technologies inter-comparison has been used.

Most measurement techniques for CO_2 use one of 4 basic approaches: gas based, electrochemical, wet-chemical or fluorescent optode analysis. A general description of each approach is presented below, with an evaluation of the potential for in situ sensing of the current technology. It is important to note, that temperature cross-sensitivity is a problem for all sensors with respect to in situ CO_2 analysis, and therefore temperature measurements alongside the CO_2 measurements are required. Calibration of sensors is typically performed with reference gases, either through direct introduction into the detector or by bubbling the gases through seawater in which the sensor is positioned (at relevant temperatures).

2.1. Gas-based pCO_2 analysis techniques

Gas-based techniques transfer seawater CO_2 into the gas phase prior to analysis. In a flow-through equilibrator system, the CO_2 is equilibrated between seawater and a gas phase, and the equilibrated gas subsequently transferred to a detector for analysis. The equilibrator design influences the water-gas exchange efficiency, and therefore determines the sensor response time. There are four main equilibrator designs: bubbler type [36], shower type [37,38], laminar flow [39] and percolated-bed [40,41]. In more recently developed silicone-based membrane equilibration systems [21,26,42], the seawater CO_2 diffuses across a semi-permeable membrane to a continuous internally circulating dry nitrogen gas stream [21,23]. Membrane-based systems can be more compact by utilising a closed gas flow system, and therefore are more suited for in situ deployment, compared with other equilibrator designs. However, pressure variations may have physical effects on membranes when deployed at depth and may influence the sensor response times [15].

An inter-comparison exercise revealed no significant differences between various pumped equilibrator types [43], although passive diffusion membranes had slower response times [44]. The same study also noted the importance of accurate equilibrator and in situ temperature measurements, with poor temperature readings giving inconsistent pCO_2 results.

Table 1

A selection of commonly used oceanic pCO_2 sensors. Where NDIR = non dispersive infrared spectroscopy, CRDS = cavity ring down spectroscopy, GC = gas chromatography, SPM = spectrophotometric, ISFET-pCO_2 = ion-selective field effect transistors to measure pCO_2, Ø is the diameter where a cylindrical housing is used, Res = Resolution, τ_{63} = time taken for the signal to reach 63% of its final value (τ_{90} is the time for a 90% response, and so forth). Numbers quoted are those from the relevant references, with the numbers in brackets converted to the same units to allow for comparison.* indicates manufacturer's specification.

Manufacturer and model	Detection type	Precision/resolution	Accuracy	Response time	Drift	Power consumption	Dimension/weight	Pressure rating and hysteresis	Range
Contros Hydro-CO$_2$ [15,21–23]	NDIR	(Res) <1 µatm*	5 µatm at surface	τ_{63} = 130–210 s (pumped)	0.15 µatm day^{-1}	1–7 W	90 Ø × 530 mm; 5.5 kg in air	2000 m	200–1000 µatm
Pro-Oceanus CO$_2$ –Pro [24–27]	NDIR	0.01 µatm	2–8 µatm (Reference dependent)	τ_{63} = 120 s (including gas equilibration, pumped)	8.7 µatm/16 days in situ	4.8–7.2 W (up to 18 wats during start up)*	190 Ø × 330 mm*; 5.5 kg*	±10–7.9 µatm; upto 2000 m*	0–2000 µatm
Picarro G2401 CRDS [28,29]	CRDS	<50 ppb (0.05 µatm)*	0.5 ppmv (0.5 µatm)	5 min (pumped)	–0.3 ppmv at 380 ppmv	260 W (start-up), 125 W Analyser*	430 × 178 × 448 mm (without pump)*; 27 kg*	Surface only	300–500 µatm*
Sunburst SAMI-CO$_2$ [30–32]	SPM	1 µatm	2 µatm	5 min (pumped)	<1 µatm/6 months*	14 A-h for 2 months	152 Ø × 550 mm*; 7.6 kg*	600 m*	200–600 µatm
Clarke et al. (in Prep.)	Optode	0.9 µatm lab	~	τ_{90} = 3 min (stirred at 20°C)	1.7 µatm/6 weeks	1.8 W	200 × 200 × 100 mm; <5 kg	Surface only	280–800 µatm
Aanderaa Optode [33]	Optode	2 µatm (over range 200–1000 µatm)	2–75 µatm	τ_{63} = 88 s at 20°C (not specified if stirred)	None detected	80 mW	36 Ø × 86 mm	6000 m; No Hysteresis detected	0–50,000 µatm
MAPCO2 [34,35]	NDIR	0.6 µmol mol^{-1} between 100 and 600 µatm (0.6 µatm)	0.3 µmol mol^{-1} (0.3 µatm)	Total sample response time 30 min (pumped)	–0.02 µmol mol^{-1} (–0.02 µatm)	243 Amp Hours (2.43-kWh)	~80 kg	Surface only	0–1000 µatm

2.1.1. GC based pCO₂ detection

Gas chromatography (GC) based pCO_2 detection was pioneered on ships in the 1970s [36,45], whereby CO_2 is extracted into an internal carrier gas stream and reduced to methane with a nickel/palladium catalyst before analysis with a flame ionising detector [36,46]. The GC technique can be used for analysis of both atmospheric and water samples, allowing determination of air-sea pCO_2 fluxes. The approach uses small air sample volumes (1 ml [37]), has a linear response over a wide range of CO_2 concentrations (250−2000 μatm [47]), and produces high quality shipboard data with a precision <0.25% [48]. However, GC requires stable temperatures, a flame, pressurised gas to move the sample through the system, an expensive catalyst for analysis, as well as large water sample volumes (200−500 ml [49]). For these reasons, the GC analysis has not been developed further into *in situ* systems.

2.1.2. NDIR spectroscopy pCO₂ detection

Non-dispersive infrared spectroscopy (NDIR) uses the characteristic vibration of gaseous CO_2 upon absorption of infrared radiation. NDIR has a non-linear response over a wide measurement range (0−3000 μatm, [50]). It is widely used for shipboard pCO_2 measurements, with increasing numbers of commercial *in situ* systems, featuring a variety of response times, precisions and concentration ranges (see Table 1).

The NDIR based systems have been deployed on buoys and moorings [51], and on commercial ships (termed ships of opportunity) which have limited sensor maintenance opportunities [41]. The latter deployments have provided high-quality and high-resolution surface ocean data along commercial shipping routes, readily available through the SOCAT website [52], and have greatly increased our understanding of spatial and temporal pCO_2 variability [26,41,53].

To correct for detector drift, regular calibration with certified reference gases is required along with daily blank measurements. The seawater-equilibrated gas must be dried (to minimise band broadening) before entering the NDIR detector. These requirements, and the limited quantification of pressure effects, have so far limited *in situ* deployments on mobile platforms [15]. Recent studies have shown that marine air can be used as an alternative reference during deployment periods in between land-based calibrations [15], or soda lime can be used to remove CO_2 from the seawater-equilibrated air-stream as an alternative blank [21].

In addition, for the best measurement precision and accuracy, the NDIR detector requires stable temperatures. The use of a heater forms a possibility to maintain a constant temperature gradient [21], however this constitutes an additional power requirement. Furthermore, variations in water temperatures can have significant effects on sensor response times, and can lead to challenges during deployments in dynamic ocean areas or on mobile platforms [15].

At present, NDIR systems produce *in situ* pCO_2 measurements at the highest accuracy and precision, and the alternative calibration and zeroing procedures facilitate *in situ* deployment of NDIR. However, the systems are typically large (Table 1), require regular drift corrections and re-calibration to ensure long-term measurement stability, have high power requirements, which all make deployment on autonomous platforms challenging.

2.1.3. Cavity ring-down spectroscopy for pCO₂ measurements

Cavity ring down spectroscopy (CRDS) utilises the absorption of light by CO_2 at a wavelength of ca. 1600 nm produced by a narrow bandwidth continuous-wave laser. Once a pre-set light intensity is reached in the mirror-lined cavity, the laser is switched off and the light decay over time is analysed with a photodiode. Increasing concentrations of CO_2 increase the light attenuation [54]. The technique can be used to measure pCO_2, as well as corresponding

isotopes ($^{12}CO_2$, $^{13}CO_2$), carbon monoxide, methane and water vapour concentrations for full characterisation of the ocean carbon cycle [28]. The technique has been used for measurements of both atmospheric and seawater CO_2 [29].

Early seawater applications showed an accuracy of 0.5 ppmv and a response time (τ_{90}) of 400 s [29], with the response time strongly influenced by the equilibrator design and water flow rate [55]. A stability of ±0.15‰ over a period of a year (without re-calibration) has been reported, which is a marked advantage compared to NDIR [54]. However, CRDS systems are bulky, have large power requirements and need stable operation temperatures [54], which makes *in situ* application challenging. Regular analyses of reference gases with well-defined methane and oxygen concentrations are required to correct for drift [29]. The systems also require the gas stream to be dried, and a correction factor applied to obtain high quality data [56]. The CRDS approach is still in its infancy with respect to oceanic pCO_2 measurements and has currently only been deployed on ships. Due to the need for regular reference gas measurements with dried gas, and the large size of the systems, they are unlikely to be used for *in situ* measurements in the near future.

2.2. Electrochemical pCO₂ systems

First introduced in 1958, the electrochemical systems consist of a glass pH electrode in a sodium bicarbonate buffer solution enclosed by a membrane [57]. The pH electrode voltage is recorded relative to a reference electrode, with any voltage change proportional to the pH change in the buffer solution, and therefore pCO_2. Recent developments have focused on the type and thickness of membrane and pH electrode design [58]. The systems allow detection of low CO_2 levels, with detection limits below 3 μM [59]. However, response times are controlled by the buffer reaction rates and diffusion distances, with times ranging from 60 s [60] to ca. 4 min [61]. The addition of carbonic anhydrase to the membrane [62,63] decreases the response time, but the enzyme is only stable at low temperatures for a period of a month [62], and may denature over longer deployments [64].

A more recent electrochemical-based system implements an Ion-Selective Field-Effect Transistor (ISFET) pH sensor with a buffer solution and membrane. A pCO_2 induced pH change in the buffer solution causes a change in the surface charge of the ISFET, and an alteration in the strength of the electric field of the internal transistor relative to a reference electrode. The initial results are promising with a response time of less than 60 s whilst deployed statically at depth and at low temperatures [65,66] but the approach has yet to be fully calibrated to determine pCO_2 directly from the voltage change [60].

The main limitation in the electrochemical systems is caused by the pH electrodes. With classical electrodes, the standard potential of the internal and external reference electrodes is both pressure and temperature sensitive [58,59], with a susceptibility to electromagnetic interferences [67]. Furthermore, the liquid junction potential drifts with the migration of highly charged seawater ions [59], and to counteract this the electrodes require regular (weekly − monthly) calibration [58]. The liquid junction potentials of the pH-ISFET have a strongly pressure dependent output, causing hysteresis, such that the sensors are not recommended for use at depth [68,69]. Classical electrode systems are not typically used for *in situ* pH or pCO_2 measurements.

Intense research efforts are underway to address issues with the pH-ISFET, however a recent deployment on an underwater glider showed poor stability and light sensitivity [70]. Despite deployments of a pCO_2-ISFET alongside a pH-ISFET system in different settings, there is little data available on the performance of the pCO_2 sensor independent of the pH-ISFET. The pCO_2-ISFET requires

careful calibration and characterisation, before it can be more fully evaluated with respect to other systems presented here.

2.3. Wet-chemical spectrophotometric pCO₂ systems

Spectrophotometric pCO_2 systems pump a colorimetric pH indicator through a CO_2 permeable tube (e.g. silicone rubber [71–74] or Teflon AF [75–77]) where it equilibrates with the seawater sample, before being propelled to the detection cell where the absorbance of the solution is measured at three wavelengths (absorbance of the acidic and conjugate base forms of the indicator, and an independent reference wavelength). Blank seawater-only solutions are measured periodically to correct for light intensity fluctuations and mitigate the effects of biofouling [78].

Commonly used pH indicators are bromothymol blue [71,72], and thymol blue [74] with hydroxypyrene-1,3,6-trisulfonic acid (HPTS) reported in a microfluidic system [76]. Precisions vary from <1 µatm [30] to 0.4% [75], with stability reported from 10,000 consecutive measurements [30] to 6 month [74]. Response times are determined (as for the electrochemical systems) by the diffusion distance of CO_2 and the reaction time with the pH indicator. These vary from minutes [71,75] up to an hour [73], while the response of the microfluidic system varies with CO_2 concentration from 1 min at 214 µatm to 3.8 min at 493 µatm [76].

There are several other potential challenges with *in situ* spectrophotometric deployments, such as light source instability, membrane or semi-permeable tubing deterioration and biofouling effects [75]. Bubbles in the system can also hinder or distort the measurements, particularly in microfluidic systems [79]. Despite these issues, the systems have been successfully deployed on moorings [71] and lagrangian buoys [74], with no significant observable drift but an offset from discrete sample measurements [32]. Deployment time for spectrophotometric systems is typically determined by battery lifetime, with SAMI-CO₂ deployed for 6 months with a 0.5 hr^{-1} analysis resolution [31]. The SAMI-CO2 was calibrated using reference gases bubbled through seawater, and using blank seawater to monitor potential drift. No drift was detected in the ACT deployment, indicating excellent potential for longer deployments [32].

Spectrophotometric pCO_2 measurements using microfluidic sensors have advantages because of their smaller size and lower reagent and power requirements [76]. Future developments may see these microfluidic systems being more widely deployed on mobile *in situ* platforms where size and power requirements form important constraints.

2.4. pCO₂ optodes

Optodes for pCO_2 measurements consist of an analyte-sensitive indicator immobilised in a gas-permeable membrane, termed sensor spot. Light from a Light Emitting Diode (LED) is directed to the spot, exciting the indicator, which emits photons and these are subsequently detected with a photodetector. The photodetector can be located either opposite the chemical spot in a flow-through system or alongside the light source.

pCO_2 optodes allow measurement of pCO_2 in the dissolved phase [76] and can be deployed directly in seawater with no reference gases nor mechanical parts, which is a significant advantage compared to the NDIR and spectrophotometric CO_2 methods. Table 2 lists a selection of pCO_2 optodes that have been used in marine systems. The majority were designed for and deployed at sediment − water interfaces where the pCO_2 gradients are pronounced.

Optodes are small and rugged with simple electronics, no wet chemicals or waste products. Response times are primarily determined by CO_2 diffusion across the membrane, and are on the order of minutes (Table 2). The thickness of the diffusive boundary layer above the membrane contributes to the response time, and this can be reduced by stirring of the solution [80].

There is no CO_2 consumption during the analysis, allowing repeated analysis in small sample volumes. To date, pCO_2 optodes have yet to be fully commercialised for water column measurements.

The potential for successful *in situ* water column deployment using optode technology (based on the success of its oxygen counterpart) merits further discussion of their designs and suggestions for future developments.

3. Optode sensor technology

3.1. Hardware

The electronic components consist of a light source, optical waveguide, and a photodetector (Fig. 1). The main variations between optode systems come from selection of the light source and photodetectors. Filters can be used to improve signal to noise ratios (SNR) of the sensor, but are not essential.

The light source must provide a stable illumination with low power consumption. LEDs and laser diodes (LD) are most commonly used due to their reliability, and small size; LEDs are preferable as they can use smaller and less stable power supplies compared to LDs [84]. LEDs are produced in a variety of wavelengths with a full width at half maximum (FWHM) of ca. 25 nm, allowing use without filters [85], and have low power requirements, thereby making them ideal for *in situ* systems.

The photoemission from the optode spot is quantified with a photodetector, which should have a high sensitivity with a fast response [86]. There is a range of suitable detectors, from small but less sensitive photodiodes, to the larger but more sensitive photon multiplier tubes (PMTs). Avalanche Photodiodes (APDs) offer intermediate performance and complexity. PMTs show a good SNR at low light levels due to their high sensitivity. Charged Coupled Devices (CCDs) linked to cameras can be used to create a planar image of the pCO_2 concentration across the surface of the spot, however they may require high quality lenses and make the systems expensive and bulky. Photodiodes are attractive for *in situ* systems as they are low cost and small, but less sensitive [87].

3.2. Spot composition

There are common approaches to the architecture of the optode spots, with different development approaches between

Table 2
Previous optodes deployed in marine environments with analysis technique, precision, response time and the desired deployment environment. Where HPTS = 8-hydroxypyrene-1, 3, 6-trisulfonic Acid, TOA = tetraoctyl-ammonium, TOA-OH = tetraoctyl ammonium hydroxide, f-DLR = frequency domain dual lifetime referencing, *t*-DLR = time domain dual lifetime referencing, FRET = fluorescence resonance energy transfer.

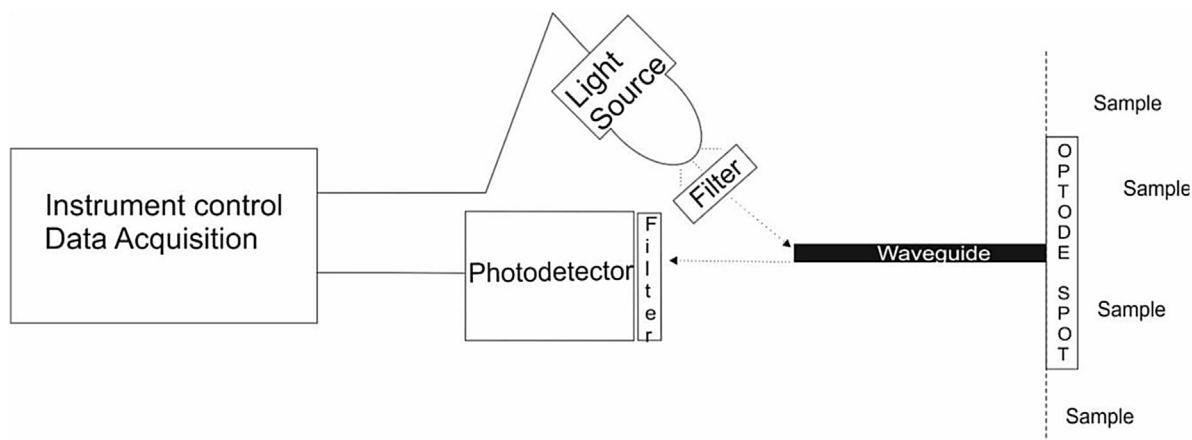| Study	Indicator and support	Analysis	Precision	Response time (unstirred)	Deployment
Schroeder, Neurauter [81]	HPTS, TOA (HCO₃) in ethyl cellulose membrane	*t*-DLR	~	~	Aquatic sediments
Zhu, Aller [82]	HPTS, TOA and TOA-OH in ethyl cellulose membrane	*f*-DLR		2.5 min	Marine sediments
Neurauter, Klimant [83]	HPTS-TOA in cellulose membrane	FRET	60 ppb	<1 min	Water-sediment interface

Fig. 1. Schematic of optode setup.

manufacturers. The three main components of the sensor spots are the support, membrane and indicator (Fig. 2). The support is in contact with the sensor hardware and typically consists of an inert strong compound such as polyethylene terephthalate [88].

3.3. Membrane

The membrane influences the immobilised indicator properties and response time of the optode. The primary considerations for membrane selection for pCO_2 measurements are gas permeability, non-fluorescent characteristics and suitable interactions with the indicator of choice. The most commonly used membranes are composed of cellulose, sol-gel, or hydrogels.

Ethyl cellulose is a widely used polymer membrane due its stability over the basic pH range and robustness with high permeability towards CO_2 [89]. Cellulose membranes suffer from ion penetration, and an additional silicone layer between the sample solution and spot may mitigate this, and additionally act as optical insulation [88].

Hydrogels (such as polyurethane hydrogels [90,91]) use covalent coupling with the indicator as opposed to the ionic interaction of ethyl cellulose. Silica sol-gels have similar features to hydrogels, but use encapsulated silica to form the membrane as opposed to linked polymers used in hydrogels. Both the curing time and starting polymers or silica used to form the hydrogels and sol-gels must be carefully chosen for the correct pore size and indicator interaction. The thickness of the membrane is a major contributor

to the CO_2 diffusion distance and therefore the response time of the sensor.

Optical isolation layers may be added to the outside of the membrane in contact with the sample. These limit potential light interferences from interactions of the LED light with components in the sample solution (e.g. chlorophyll), and interference from sunlight, thereby improving the measurement quality. A suitable material for optical isolation is Teflon AF™, due to its low refractive index and high gas permeability with no water transfer. Silicone rubber is also suitable due to its excellent adhesion, chemical inertness and high gas permeability. The optical isolation layer slows the sensor response time by increasing the CO_2 diffusion distance.

3.4. Indicators

Desirable characteristics for the indicator include stability upon immobilisation, a detection range suitable for the pCO_2 levels in seawaters, and a low photo-bleaching rate. Fluorescent pH indicators are in common use for pCO_2 optodes due to the range of suitable, characterised indicators available across the marine pH range. Molecules in use include the pH indicators 1-hydroxy-3,6,8-pyrenetrisulfonic acid (HPTS) [82,92,93], the diazo dye Sudan III [94] and diketo-pyrrolo-pyrolle (DPP) [95]. The use of pH indicators further requires the immobilisation of a buffer molecule to cause the change in pH upon pCO_2 variations, and hence yield a fluorescence response from the indicator.
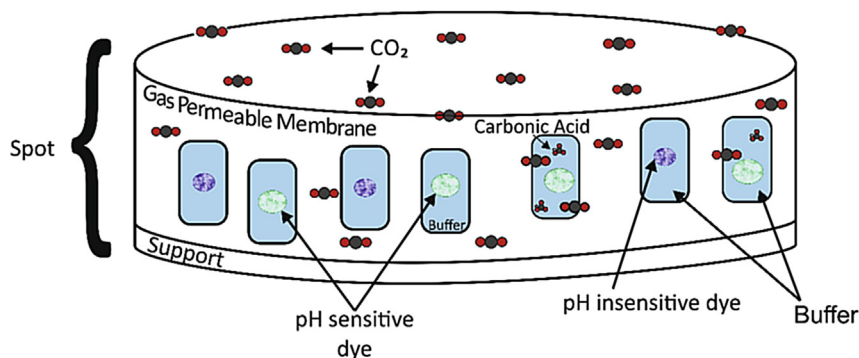

Fig. 2. Generalised pCO_2 spot composition. The gas permeable membrane is in contact with the solution. The CO_2 molecules diffuse across the membrane and interact with the buffer solutions (denoted by the blue rectangles) and form carbonic acid which in turn interacts with the pH sensitive dye (the green circles) causing a change in the fluorescence signal. The pH insensitive dye is not influenced by the carbonic acid and provides a constant background fluorescence signal. The support is made of a strong, transparent inert compound and is attached to the fibre optic cable.

An anion stabiliser is often immobilised alongside the indicator, creating an ion-pair which mitigates indicator leaching [96]. This stabiliser can also be used as the immobilised buffer. The most common molecule used for this purpose are quaternary ammonium hydroxides, e.g. tetraoctylammonium (TOA). HPTS —TOA is the most widely used pH-ion pair combination in pCO_2 optodes [83,97,98] due to the high sensitivity, high photostability (under illumination at 460 nm [99]) and an excellent quantum yield [100]. From here on, the analyte-sensitive indicator refers to the combination of pH indicator with a buffer molecule as opposed to a directly CO_2 sensitive molecule.

Depending on the intended analysis method (see section 3.5), an analyte-insensitive indicator may also be immobilised alongside the analyte sensitive indicator. These must have similar absorption and emission spectra to the analyte-sensitive indicator.

3.5. Analysis methods

There are three main techniques for signal detection in optode systems: fluorescence intensity, fluorescent resonance energy transfer (FRET) [89] and dual luminophore referencing (DLR) [101], with the ratiometric DLR further subdivided between frequency and time domain approaches (f-DLR and t-DLR, respectively). The technique selected will have some bearing on the chemistry of the sensing spot.

Fluorescence intensity measurements simply record, upon excitation, the total fluorescence response at a specific wavelength. These measurements are largely obsolete with the implementation of fluorescence reference molecules (see below) which eliminate interferences caused by e.g. sample turbidity and light source fluctuations [102].

3.5.1. FRET

For FRET analysis, a CO_2 insensitive donor complex luminesces upon excitation with light and transfers energy to a colorimetric pH dependant absorber that has a good absorption spectrum overlap with the fluorescence emission spectrum of the donor complex. At increasing CO_2 (and therefore decreasing pH), the pH dependent absorber becomes protonated and the overlap diminishes, giving the CO_2 insensitive donor complex a longer fluorescence lifetime. The lifetime is measured through a change in the phase angle of a single modulation frequency signal [94].

FRET allows integration with existing oxygen sensor technology, thereby reducing the sensor development and production costs [89]. A sensor applying the FRET technique (Table 2) has a rapid response time of 24 s for 99% of the final value (τ_{99}) with a tuneable sensitivity. The pCO_2 optodes using FRET show however a cross-sensitivity towards oxygen due to the use of a ruthenium compound as the luminescence donor. This method has lower SNR ratios, but an enhanced susceptibility to signal drift compared to the DLR techniques.

3.5.2. f-DLR

The DLR technique requires two molecules to fluoresce with different lifetimes: a reference dye with a relatively long lifetime (microseconds) and an indicator molecule with a short lifetime (nanoseconds) [102]. The f-DLR technique uses the change in phase angle caused by a change in the ratio of the fluorescence signal amplitude of the indicator and reference molecules. The reference fluorophore provides a background fluorescence signal that is not affected by changes in pCO_2; the major change in the phase angle comes from the change in the pCO_2 sensitive indicator fluorescence.

Recent work has shown the suitability pCO_2 optode spots for f-DLR based monitoring [103]. The setup achieved a precision of ±2 μatm over a CO_2 range of 200—1000 μatm and a response time

(τ_{63}) of 88 s at 20°C. The system has no moving mechanical parts or chemical reagents, but is irreversibly poisoned by hydrogen sulphide.

3.5.3. t-DLR

The DLR technique can also be used in the time domain approach (t-DLR). In this case both reference and indicator molecules are excited using the same wavelength and the intensity is integrated through two 'time windows' (Fig. 3). One window is during the molecular excitation where the response is controlled by the strong fluorescence from the pCO_2 sensitive dye, and the other window is during the fluorescence decay where the response is mostly attributed to the pCO_2 insensitive long lifetime dye. The ratio of the integration of the windows can be directly related to pCO_2. This method has similar disadvantages to the f-DLR technique such as potential drift from photo-bleaching of the indicator and reference dyes at different rates. However, the use of time windows allows shorter excitation times of the spot, and results in reduced photo-bleaching and increased spot longevity.

4. Optode pCO_2 for open ocean observations

A pCO_2 t-DLR optode was characterised and deployed as an underway shipboard system for high-resolution measurements of oceanic surface waters (Fig. 4). The spot was illuminated with a blue (475 nm) LED at low intensity to minimise power requirements (1.8 W for the whole system) and spot bleaching. The time taken to achieve 90% of the final pCO_2 value (τ_{90}) was determined as 160 s at 25°C, with a laboratory precision of 0.8 μatm (n = 10 in certified reference seawater from Andrew Dickson, batch 144, 20°C). An initial calibration over 290—450 μatm at 25°C and seawater salinity (35) was performed using a gas calibration rig [105].

The preliminary pCO_2 optode deployment was over a period of 6 weeks, measuring once per 6 min, from the Labrador Sea to the Iceland Basin in the North Atlantic. This shipboard deployment allowed rigorous testing of the lifetime and drift of the spot in changing oceanographic environments while maintaining a consistent experimental laboratory set-up.

To account for and quantify any potential drift, certified reference materials (CRMs) for TA and DIC, obtained from Prof. A. Dickson (Scripps, USA), were analysed weekly. These measurements showed a drift of 1.7 μatm over the 6 week cruise and provided a long-term shipboard precision of 9.5 μatm (n = 64,
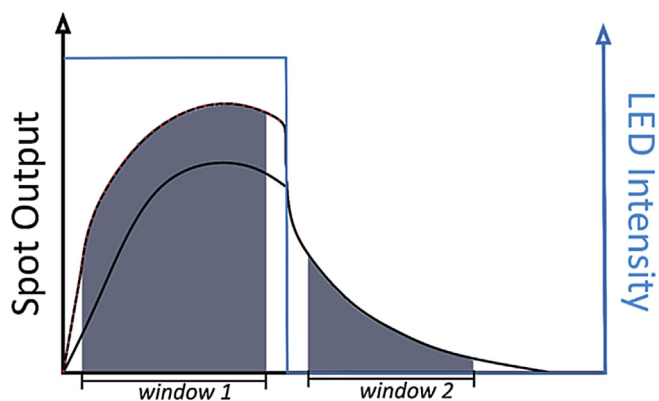

Fig. 3. LED waveform (blue square lines) with the spot output (black shark fin curves from the reference dye, and the red and black dashed line from the pCO_2 sensitive dye) analysed by t-DLR. Window 1 records the fluorescence while the LED is on and the response is primarily from the pCO_2 sensitive dye (red and black), and Window 2 records the fluorescence decay while the LED is off, attributed primarily to the longer decay lifetime of the reference dye (black line) [104].
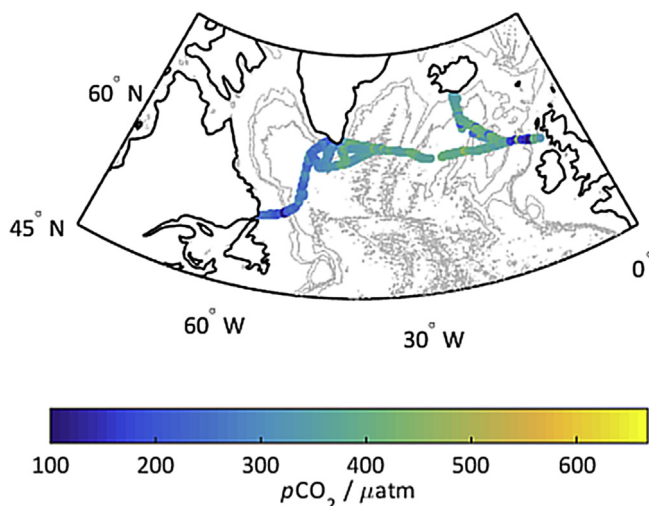
Fig. 4. Shipboard deployment of a pCO_2 optode spot using the t-DLR analysis technique over a period of 7 weeks, with initial pCO_2 concentration denoted by the coloured points overlaid on the cruise track.

standard deviation of the standards). The CRM bottles were used immediately after opening, and the optode was submerged at the bottom of the bottles, which were subsequently closed to limit CO_2 exchange with the atmosphere. Three measurements were undertaken in the individual CRM bottles, before being discarded. It was assumed that the pCO_2 in the bottles was within the calculated error for pCO_2 (6 µatm) as determined using CO_2SYS from the certified DIC and TA concentrations. The optode response was further verified using discretely collected surface seawater samples which were analysed using standard laboratory DIC and TA reference techniques, as per Atamanchuk et al. 2015 [103].

The weaker ship-based relative to laboratory precision may have resulted from stronger microbial interferences during the oceanographic deployment, potentially from microbial fouling of the optode spot surface. The pCO_2 ranged from 150 µatm in the Labrador Sea to 500 µatm in the eastern North Atlantic. The lower pCO_2 in the Labrador Sea was due to the CO_2 uptake by phytoplankton during the spring bloom [106] (Fig. 4). The Labrador Sea has an earlier spring bloom compared to the eastern North Atlantic as early in the season polar water masses transport nutrient-rich, low salinity waters to the Labrador Sea, thereby providing good light and nutrient conditions to stimulate phytoplankton growth. The phytoplankton bloom progresses east during spring, reducing surface water pCO_2 levels. Our pCO_2 results and the sensor performance will be discussed in more detail in a future publication. As is the case for the f-DLR based optode, the t-DLR optode deployed in the North Atlantic had a strong temperature dependence with limited salinity dependence, and calibration algorithms were used to correct for this.

5. Summary and future outlooks

At present, the NDIR pCO_2 sensors constitute the most developed technology for *in situ* measurements in ocean waters, but require CO_2 to be in the gas phase for analysis and suffer from spectrometer drift. The NDIR pCO_2 sensors have been deployed on moorings, buoys and mobile platforms, but further work is required to reduce their response time and gas calibration frequency to facilitate extended routine deployments on mobile platforms. The pCO_2-ISFET sensor shows promising initial results but further calibration and laboratory testing are required before a more robust evaluation can be provided. The wet-chemical spectrophotometric

techniques have volume and pCO_2 dependent response times and require minimal *in situ* calibration. Further development of suitable reference materials is recommended, particularly for the new generation sensors that analyse pCO_2 in the aqueous phase. Reference gases provide high accuracy measurements but cannot be used for *in situ* measurements, in particularly at depth. Regular *in situ* calibration with reference seawater materials during deployment of the sensors would form a good solution. Initial work on the use of DIC-TA reference materials for pCO_2 calibration showed promise [107], although further work is required.

The work presented indicates the suitability of pCO_2 optodes for open ocean measurements. The optodes have a low power requirement, no moving mechanical parts, and require no reagents and produce no waste. The pCO_2 optodes hence show great potential for application on floats, gliders and moorings, with future applications envisaged in monitoring oceanic and coastal waters, and e.g. in industrial scenarios of CO_2 leak detection in the vicinity of carbon capture and storage sites. Current optode spot developments are focussed on decreasing response times, reducing salinity dependency, and enhancing stability. Optode spot design is also progressing towards multiple analyte determinations with combinations such as pCO_2, O_2, pH, and/or temperature within a single sensing spot [81]. This will be a significant advantage on mobile platforms where space, weight and power are limited. However, optodes are still in the early stages of development with further developments and *in situ* testing required before they can compete with the NDIR technique.

Acknowledgements

References

[1] Scripps, The Keeling Curve, vol. 25, May 2016. Available from: https://scripps.ucsd.edu/programs/keelingcurve/.
[2] C. Le Quéré, et al., Global carbon budget 2014, Earth Syst. Sci. Data 7 (1) (2015) 47–85.
[3] S.C. Doney, et al., Surface-ocean CO_2 variability and vulnerability, Deep Sea Res. Part II Top. Stud. Oceanogr. 56 (8–10) (2009) 504–511.
[4] C. Le Quéré, et al., Trends in the sources and sinks of carbon dioxide, Nat. Geosci. 2 (2009) 831–836.
[5] F.J. Millero, The marine inorganic carbon cycle, Chem. Rev. 107 (2) (2007) 308–341.
[6] S.C. Doney, et al., Ocean acidification: the other CO_2 problem, Ann. Rev. Mar. Sci. 1 (2009) 169–192.
[7] N.L. Bindoff, et al., Observations: oceanic climate change and sea level, in: S. Solomon, et al. (Editors), Contribution of Working Group I to the Fourth Assessment Report of the Intergovernmental Panel on Climate Change, Cambridge University Press, Cambridge, United Kingdom and New York, NY, USA, 2007, pp. 385–432.
[8] J.E. Dore, et al., Physical and biogeochemical modulation of ocean acidification in the central North Pacific, Proc. Natl. Acad. Sci. U. S. A. 106 (30) (2009) 12235–12240.
[9] R.J. Woosley, F.J. Millero, R. Wanninkhof, Rapid anthropogenic changes in CO2and pH in the atlantic ocean: 2003-2014, Glob. Biogeochem. Cycles (2016) p. n/a-n/a.
[10] N.R. Bates, et al., Detecting anthropogenic carbon dioxide uptake and ocean acidification in the North Atlantic Ocean, Biogeosci. Discuss. 9 (1) (2012) 989–1019.
[11] H. Thomas, et al., Rapid decline of the CO_2 buffering capacity in the North Sea and implications for the North Atlantic ocean, Glob. Biogeochem. Cycles 21 (4) (2007).
[12] G.M. Marion, et al., pH of seawater, Mar. Chem. 126 (1–4) (2011) 89–96.
[13] R.H. Byrne, Measuring ocean acidification: new technology for a new era of ocean chemistry, Environ. Sci. Technol. 48 (10) (2014) 5352–5360.
[14] C.C. Eriksen, et al., Seaglider: a long-range autonomous underwater vehicle for oceanographic research, IEEE J. Ocean. Eng. 26 (4) (2001) 424–436.
[15] B. Fiedler, et al., In situ CO_2 and O_2 measurements on a profiling float, J. Atmos. Ocean. Technol. 30 (1) (2013) 112–126.

[16] R.H. Byrne, et al., Sensors and systems for in situ observations of marine carbon dioxide system variables, in: J. Hall, D.E. Harrison, D. Stammer (Editors), OceanObs '09: Sustained Ocean Observations and Information for Society, 2010. ESA Publication WPP-306: Venice, Italy.

[17] K. Johnson, et al., Observing biogeochemical cycles at global scales with profiling floats and gliders, Oceanography 22 (3) (2009) 216–225.

[18] T.R. Martz, et al., Technology for ocean acidification research needs and availability, Oceanography 28 (2) (2015) 40–47.

[19] G.A. Mills, G. Fones, A review of in situ methods and sensors for monitoring the marine environment, Sens Rev. 32 (1) (2011).

[20] M.N. Tamburri, et al., Alliance for coastal technologies: advancing moored pCO$_2$ instruments in coastal waters, Mar. Technol. Soc. J. 45 (1) (2011) 43–51.

[21] P. Fietzek, et al., In situ quality assessment of a novel underwater pCO$_2$ sensor based on membrane equilibration and NDIR spectrometry, J. Atmos. Ocean. Technol. 31 (1) (2014) 181–196.

[22] D. Schar, et al., Performance demonstration statement contros HydroC/CO$_2$, in: UMCES Technical Report Series, Alliance for Coastal Technologies, 2009.

[23] Contros Systems & Solutions, HydroC™ CO$_2$ Carbon Dioxide Sensor, 2015.

[24] CO$_2$-Pro, Pro Oceanus, 2015. Available from: http://www.pro-oceanus.com/co2-pro.php.

[25] D. Schar, et al., Performance demonstration statement pro-oceanus system inc, CO$_2$-pro, in: UMCES Technical Report Series, Alliance for Coastal Technologies, 2009.

[26] Z.-p. Jiang, et al., Application and assessment of a membrane-based pCO$_2$ sensor under field and laboratory conditions, Limnol. Oceanogr. Methods 12 (2014) 264–280.

[27] Z.-p. Jiang, Variability and control of the surface ocean carbonate system observed from ships of oppertunity, in: School of Ocean and Earth Science, University of Southampton, 2014, p. 165.

[28] Picarro Inc. Picarro G2201 Analyzer [2015 18/02/2015]; Available from: http://www.picarro.com/products_solutions/isotope_analyzers/13c_for_ch4_co2.

[29] M. Becker, et al., Using cavity ringdown spectroscopy for continuous monitoring of d^{13}C(CO$_2$) and fCO$_2$ in the surface ocean, Limnol. Oceanogr. Methods 10 (2012) 752–766.

[30] Sunburst Sensors LLC. SAMI-CO$_2$ Ocean CO$_2$ Sensor. [cited 2014 29/10/2014]; Available from: http://www.sunburstsensors.com/products/oceanographic-carbon-dioxide-sensor.html.

[31] M.D. DeGrandpre, M.M. Baehr, T.R. Hammar, Calibration-Free optical chemical sensor, Anal. Chem. 71 (1999) 1152–1159.

[32] D. Schar, et al., Performance demonstration statement sunburst sensors SAMI-CO$_2$, in: UMCES Technical Report Series, Alliance for Coastal Technology, 2009.

[33] D. Atamanchuk, et al., Performance of a lifetime-based optode for measuring partial pressure of carbon dioxide in natural waters, Limnol. Oceanogr. Methods 12 (2014) 63–73.

[34] A.J. Sutton, et al., A high-frequency atmospheric and seawater pCO2 data set from 14 open-ocean sites using a moored autonomous system, Earth Syst. Sci. Data 6 (2014) 353–366.

[35] D. Schar, et al., Performance demonstration statement PMEL MAPCO$_2$/battelle seaology pCO$_2$ monitoring system, in: UMCES Technical Report Series, Alliance for Coastal Technologies, 2009.

[36] C. Goyet, et al., Distribution of carbon dioxide partial pressure in surface waters of the Southwest Indian Ocean, Tellus 43B (1991) 1–11.

[37] R.F. Weiss, Determinations of carbon dioxide and methane by dual catalyst flame ionization chromatography and nitrous oxide by electron capture chromatography, J. Chromatogr. Sci. 19 (12) (1981) 611–616.

[38] H.Y. Inoue, CO$_2$ exchange between the atmosphere and the ocean, in: N. Handa, E. Tanoue, T. Hama (Editors), Dynamics and Characterization of Marine Organic Matter, Terra Scientific Publishing Company, Tokyo, Japan, 1998.

[39] A. Poisson, et al., Variability of sources and sinks of CO$_2$ in the western Indian and southern oceans during the year 1991, J. Geophys. Res. 98 (C12) (1993) 22759–22778.

[40] D.J. Cooper, A.J. Watson, R.D. Ling, Variation of P$_{CO2}$ along a North Atlantic shipping route (U.K. to the Caribbean): a year of automated observations, Mar. Chem. 60 (1998) 147–164.

[41] U. Schuster, A.J. Watson, A variable and decreasing sink for atmospheric CO$_2$ in the North Atlantic, J. Geophys. Res-Oceans 112 (C11) (2007).

[42] H. Saito, et al., A compact seawater pCO$_2$ measurement system with membrane equilibrator and nondispersive infrared gas analyzer, Deep-Sea Res. I 42 (11/12) (1995) 2025–2033.

[43] A. Körtzinger, et al., The international at-sea intercomparison of fCO$_2$ systems during the R/V Meteor cruise 36/1 in the North Atlantic ocean, Mar. Chem. 72 (2000) 171–192.

[44] I.R. Santos, D.T. Maher, B.D. Eyre, Coupling automated radon and carbon dioxide measurements in coastal waters, Environ. Sci. Technol. 46 (14) (2012) 7685–7691.

[45] R.F. Weiss, F.A. Van Woy, P.K. Salameh, in: R.J. Sepanski (Editors), Surface Water and Atmospheric Carbon Dioxide and Nitrous Oxide Observations by Shipboard Automated Gas Chromatography: Results from Expeditions between 1977 and 1990, Scripps Institution of Oceanography: Environmental Sciences Division Publication, 1992.

[46] R.H. Wanninkhof, M. Knox, Chemical enhancement of CO$_2$ exchange in natural waters, Limnol. Oceanogr. 41 (4) (1996) 689–697.

[47] A.G. Dickson, C.L. Sabine, J.R. Christian, Recommended standard operating procedure- SOP 4 : determination of p(CO$_2$) in air that is in equilibrium with a discrete sample of seawater, in: A.G. Dickson, C.L. Sabine, J.R. Christian (Editors), Guide to Best Practices for Ocean CO$_2$ Measurements, PICES Special Publication, 2007.

[48] U. Schuster, et al., Sensors and instruments for oceanic dissolved carbon measurements, Ocean Sci. 5 (4) (2009) 547–558.

[49] T. Takahashi, et al., Seasonal variation of CO$_2$ and nutrients in the high-latitutde surface oceans- A comparative study, Glob. Biogeochem. Cycles 7 (4) (1993) 843–878.

[50] M. Frankignoulle, A.V. Borges, Direct and indirect pCO$_2$ measurements in a wide range of pCO$_2$ and salinity V alues (the scheldt estuary), Aquat. Geochem. 7 (2001) 267–273.

[51] P. Fietzek, A. Körtzinger, Optimization of a membrane-based NDIR sensor for dissolved carbon dioxide, in: OceanObs'09, OceanObs'09, Venice, Italy, 2009.

[52] D.C.E. Bakker, et al., An update to the surface ocean CO$_2$ atlas (SOCAT version 2), Earth Syst. Sci. Data 6 (2013) 1–22.

[53] H. Lüger, D.W.R. Wallace, A. Kortzinger, The pCO$_2$ variability in the mid-latitude North Atlantic Ocean during a full annual cycle, Glob. Biogeochem. Cycles 18 (3) (2004).

[54] G. Friedrichs, et al., Toward continuous monitoring of seawater ^{13}CO$_2$/^{12}CO$_2$ isotope ratio and pCO$_2$: performance of cavity ringdown spectroscopy and gas matrix effects, Limnol. Oceanogr. Methods 8 (2010) 539–551.

[55] J.R. Webb, D.T. Maher, I.R. Santos, Automated, in situ measurements of dissolved CO$_2$, CH$_4$, and δ^{13}C values using cavity enhanced laser absorption spectrometry: comparing response times of air-water equilibrators, Limnol. Oceanogr. Methods (2016) p. n/a–n/a.

[56] H. Nara, et al., Effect of air composition (N$_2$, O$_2$, Ar, and H$_2$O) on CO$_2$ and CH$_4$ measurement by wavelength-scanned cavity ring-down spectroscopy: calibration and measurement strategy, Atmos. Meas. Tech. 5 (11) (2012) 2689–2701.

[57] J.W. Severinghaus, A.F. Bradley, Electrodes for blood pO$_2$ and pCO$_2$ determination, J. Appl. Physiol. 13 (3) (1958) 515–520.

[58] J. Zosel, et al., The measurement of dissolved and gaseous carbon dioxide concentration, Meas. Sci. Technol. 22 (7) (2011) 072001.

[59] M. Taillefert, G.W. Luther III, D.B. Nuzzio, The application of electrochemical tools for in situ measurements in aquatic systems, Electroanalysis 6 (2000) 401–412.

[60] K. Shitashima, et al., Development of in-situ pH-pCO$_2$ sensor for deep-sea oceanography applications, in: Sensors, 2008 IEEE, IEEE, Lecce, 2008, pp. 1414–1417.

[61] T. Ishiji, et al., Amperometric sensor for monitoring of dissolved carbon dioxide in seawater, Sens Actuators B 76 (2001) 265–269.

[62] P. Zhao, W.-J. Cai, An improved potentiometric pCO$_2$ microelectrode, Anal. Chem. 69 (1997) 5052–5058.

[63] J.H. Shin, et al., A Planar pCO$_2$ sensor with enhanced electrochemical properties, Anal. Chem. 72 (18) (2000) 4468–4473.

[64] M.B. Tabacco, et al., An autonomous sensor and telemetry system for low-level pCO$_2$ measurements in seawater, Anal. Chem. 71 (1) (1999) 154–161.

[65] D. Atamanchuk, et al., Detection of CO$_2$ leakage from a simulated sub-seabed storage site using three different types of pCO$_2$ sensors, Int. J. Greenh. Gas Control 38 (2015) 121–134.

[66] K. Shitashima, Evolution of compact electrochemical in-situ pH-pCO$_2$ sensor using ISFET-pH electrode, Oceans 1 (4) (2010) 20–23.

[67] V.M.C. Rérolle, et al., Seawater-pH measurements for ocean-acidification observations, TrAC Trends Anal. Chem. 40 (2012) 146–157.

[68] T.R. Martz, J.G. Connery, K.S. Johnson, Testing the Honeywell Durafet for seawater pH applications, Limnol. Oceanogr. Methods 8 (2010) 172–184.

[69] P.J. Bresnahan, et al., Best practices for autonomous measurement of seawater pH with the Honeywell Durafet, Methods Oceanogr. 9 (2014) 44–60.

[70] M.P. Hemming, J. Kaiser, K.J. Heywood, D.C.E. Bakker, K. Shitashima, G. Lee, O. Legge, R. Onken, Measuring pH variability using an experimental sensor on an underwater glider, Ocean Sci. Discuss. (2016), http://dx.doi.org/10.5194/os-2016-78 (in review).

[71] M.D. DeGrandpre, et al., In situ measurements of seawater pCO$_2$, Limnol. Oceanogr. 40 (5) (1995) 969–975.

[72] M.D. DeGrandpre, Measurement of seawater pCO$_2$ using a renewable-reagent fiber optic sensor with colorimetric detection, Anal. Chem. 65 (4) (1993) 331–337.

[73] N. Lefevre, et al., A new optical sensor for PCO$_2$ measurements in seawater, Mar. Chem. 42 (1993) 189–198.

[74] E.M. Hood, L. Merlivat, Annual to interannual variations of fCO$_2$ in the northwestern Mediterranean Sea: results from hourly measurements made by CARIOCA buoys, 1995-1997, J. Mar. Res. 59 (2001).

[75] Z. Lu, et al., A high precision, fast response, and low power consumption in situ optical fiber chemical pCO$_2$ sensor, Talanta 76 (2008) 353–359.

[76] X. Ge, et al., A low-cost fluorescent sensor for pCO$_2$ measurements, Chemosensors 2 (2) (2014) 108–120.

[77] Y. Nakano, et al., Simultaneous vertical measurements of in situ pH and CO$_2$ in the sea using spectrophotometric profilers, J. Oceanogr. 62 (2006) 71–81.

[78] T.S. Moore, et al., Sea surface pCO$_2$ and O$_2$ in the Southern Ocean during the austral fall, 2008, J. Geophys. Res. 116 (2011).

[79] V.M.C. Rérolle, et al., Development of a colorimetric microfluidic pH sensor for autonomous seawater measurements, Anal. Chim. Acta 786 (5) (2013) 124–131.

[80] H.C. Bittig, et al., Time response of oxygen optodes on profiling platforms and its dependence on flow speed and temperature, Limnol. Oceanogr. Methods 12 (8) (2014) 617—636.
[81] C. Schroeder, G. Neurauter, I. Klimant, Luminescent dual sensor for time-resolved imaging of pCO$_2$ and pO$_2$ in aquatic systems, Microchim. Acta 158 (2007) 205—218.
[82] Q. Zhu, R.C. Aller, Y. Fan, A new ratiometric, planar fluorosensor for measuring high resolution, two-dimensional pCO$_2$ distributions in marine sediments, Mar. Chem. 101 (1—2) (2006) 40—53.
[83] G. Neurauter, I. Klimant, O.S. Wolfbeis, Fiber-optic microsensor for high resolution pCO$_2$ sensing in marine environment, Fresenius J. Anal. Chem. 366 (2000) 481—487.
[84] M.N. Taib, R. Narayanaswamy, Solid-state instruments for optical fibre chemical sensors, Analyst 120 (1995) 1617—1625.
[85] P.C. Hauser, T.W.T. Rupasinghe, N.E. Cates, A Multi-wavelength photometer based on light-emitting diodes, Talanta 42 (4) (1995).
[86] B. Kuswandi, R. Andres, R. Narayanaswamy, Optical fibre biosensors based on immobilised enzymes, Anal 126 (8) (2001) 1469—1491.
[87] G.F. Knoll, Photomultiplier tubes and photodiodes, in: D. Matteson, J. Welter, A. Spicehandler (Editors), Radiation Detection and Measurement, Hamilton Printing Company, United States of America, 2010.
[88] B.H. Weigl, O.S. Wolfbeis, Sensitivity studies on optical carbon dioxide sensors based on ion pairing, Sens Actuators B 28 (1995) 151—156.
[89] G. Neurauter, I. Klimant, O.S. Wolfbeis, Microsecond lifetime-based optical carbon dioxide sensor using luminescence resonance energy transfer, Anal. Chim. Acta 382 (1—2) (1999) 67—75.
[90] H. Stahl, et al., Time-resolved pH imaging in marine sediments with a luminescent planar optode, Limnol. Oceanogr. Methods 4 (2006) 336—345.
[91] S.M. Borisov, R. Seifner, I. Klimant, A novel planar optical sensor for simultaneous monitoring of oxygen, carbon dioxide, pH and temperature, Anal. Bioanal. Chem. 400 (8) (2011) 2463—2474.
[92] C.-S. Chu, Y.-L. Lo, Fiber-optic carbon dioxide sensor based on fluorinated xerogels doped with HPTS, Sens Actuators B 129 (2008) 120—125.
[93] O. Oter, et al., Emission-based optical carbon dioxide sensing with HPTS in green chemistry reagents: room-temperature ionic liquids, Anal. Bioanal. Chem. 386 (2006) 1225—1234.

[94] C. Von Bültzingslöwen, et al., Lifetime-based optical sensor for high-level pCO$_2$ detection employing fluorescence resonance energy transfer, Anal. Chim. Acta 480 (2) (2003) 275—283.
[95] S. Schutting, et al., New highly fluorescent pH indicator for ratiometric RGB imaging of pCO$_2$, Methods Appl. Fluoresc. 2 (2) (2014) 024001.
[96] B. Muller, P.C. Hauser, Fluorescence optical sensor for low concentrations of dissolved carbon dioxide, Anal 121 (3) (1996) 339.
[97] O. Oter, K. Ertekin, S. Derinkuyu, Ratiometric sensing of CO$_2$ in ionic liquid modified ethyl cellulose matrix, Talanta 76 (3) (2008) 557—563.
[98] K. Ertekin, et al., Characterization of a reservoir-type capillary optical microsensor for pCO$_2$ measurements, Talanta 59 (2003) 261—267.
[99] H. Offenbacher, O.S. Wolfbeis, E. Furlinger, Fluorescence optical sensors for continuous determination of near-neutral pH values, Sens Actuators 9 (1) (1986) 73—84.
[100] C. Schröder, Luminescent planar single and dual optodes for time-resolved imaging of pH, pCO$_2$ and pO$_2$ in marine systems, in: Fakultät für Chemie und Pharmazie, Universität Regensburg, 2006.
[101] C.S. Burke, et al., Development of an optical sensor probe for the detection of dissolved carbon dioxide, Sens Actuators B Chem. 119 (1) (2006) 288—294.
[102] I. Klimant, et al., Dual lifetime referencing (DLR) - a new scheme for converting fluorescence intensity into a frequency-domain or time-domain information, in: B. Valeur, J.-c. Brochon (Editors), New Trends in Fluorescence Spectroscopy :applpications to Chemical and Life Science, Springer-Verlag, Germany, 2001, pp. 257—274.
[103] D. Atamanchuk, et al., Continuous long-term observations of the carbonate system dynamics in the water column of a temperate fjord, J. Mar. Syst. 148 (2015) 272—284.
[104] C. Schröder, B.M. Weidgans, I. Klimant, pH Fluorosensors for use in marine systems, Analyst 130 (6) (2005) 907—916.
[105] M. Sosna, et al., Development of a reliable microelectrode dissolved oxygen sensor, Sens Actuators B Chem. 123 (1) (2007) 344—351.
[106] A. Olsen, et al., Sea-surface CO$_2$ fugacity in the subpolar North Atlantic, Biogeosciences 5 (2008) 535—547.
[107] C. Neill, et al., Accurate headspace analysis of fCO$_2$ in discrete water samples using batch equilibration, Limnol. Oceanogr. 42 (8) (1999) 1774—1783.